nature

https://doi.org/10.1038/s41586-020-2190-3

Supplementary information

Tail-propelled aquatic locomotion in a theropod dinosaur

In the format provided by the authors and unedited

Nizar Ibrahim✉, Simone Maganuco, Cristiano Dal Sasso, Matteo Fabbri, Marco Auditore, Gabriele Bindellini, David M. Martill, Samir Zouhri, Diego A. Mattarelli, David M. Unwin, Jasmina Wiemann, Davide Bonadonna, Ayoub Amane, Juliana Jakubczak, Ulrich Joger, George V. Lauder & Stephanie E. Pierce✉

Supplementary Information Ibrahim et al., (2020)

"Tail-propelled aquatic locomotion in a theropod dinosaur"

This PDF file includes:

Supplementary text

1. Geological context

General

Spinosaurus aegyptiacus FSAC-KK 118887 was discovered in- and ex-situ on the slopes of a south-east facing escarpment (Supplementary Information Figure 1) fringing the Aferdou Zrigat (Ikhf n Taqmout on some maps) plateau (itself an isolated mesa of the more extensive Jbel Al Marka plateau). This locality lies on the northern margin of the extensive Tafilalt basin, which is rimmed on its north, east and south-eastern margins by an escarpment of marine limestones of the Akrabou Formation overlying the fluvio-lacustrine Kem Kem beds[45,46,47]. These well-bedded strata are of late Early to early Late Cretaceous age, and rest with angular, and gently topographic unconformity on folded Palaeozoic strata of Siluro-Devonian and Carboniferous age (the former being remarkably fossiliferous). The Cretaceous strata are horizontal, well jointed, and rendered conspicuous by their red colours at the base and cream colours at the top. Boulders and scree of the Akrabou Formation limestones unfortunately blanket much of the outcrop of the underlying Kem Kem beds (Supplementary Information Figure 1). Nevertheless, there are many excellent exposures of the Kem Kem beds in the Tafilalt, and this locality is one of several in the northern margin of the basin that yields a rich and diverse vertebrate fossil assemblage.

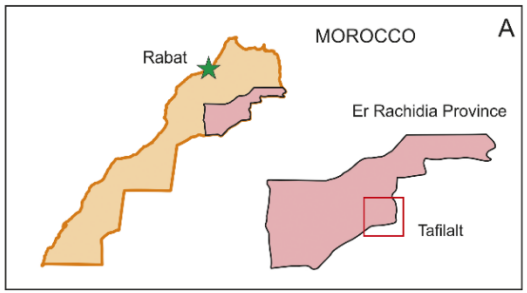

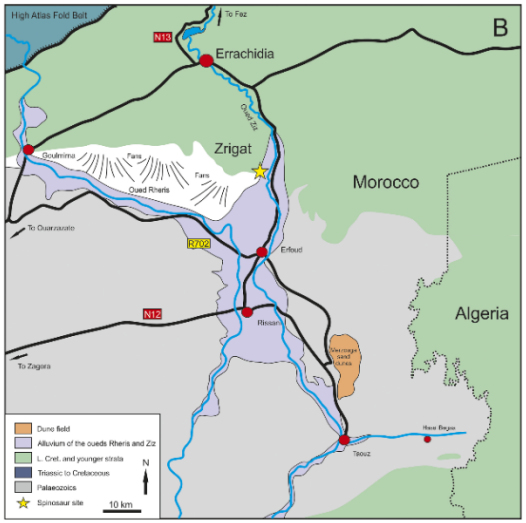

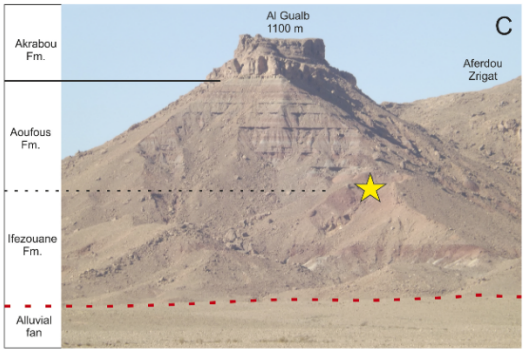

Mainly micritic limestone with some marly limestone. Highly fossiliferous with large gastropods, bivalves including rudists, oysters and heterodonts, echinoderms and rare ammonites.
The distinctive Cenomanian ammonite *Neolobites vibrayeanus* occurs infrequently.

Muddy sandstones, usually fine, passing up into silt mudstones and variegated mudstones. Thin sandstone 'event' horizons may have dinosaur footprints at some localities. Pedogenic structures and rhizoliths may be frequent towards the top. The *Spinosaurus* specimen is from this unit.

Fine to medium sands. Cross and planar bedded. Localised hiatus horizons with mud-flake conglomerates. Some low angle channels. Rare high-angle channels. Isolated vertebrate remains can be abundant in the event horizons.

Heterolithic sequence, with thin limestones. Rare diminutive bivalves, cf. *Corbula* sp. *sensu lato*.

Medium sandstones, cross and planar bedded. Well cemented, often concretionary, dark brown. Unfossiliferous.

Gently folded Palaeozoic basement. Various lithologies, including limestones, sandstones and black-shales depending on location.

Supplementary Information Figure S1. A, B) Location of Errachidia Province in Morocco and geological/geographical context of the *Spinosaurus* site near Zrigat (also spelled Zrigate). C) The inselberg of Al Gualb (1100 m) looking west with Aferdou Zrigat behind. The star highlights the level, but not the locality, of the *Spinosaurus* dig site. D) Simplified stratigraphic scheme for the Zrigat area of the Tafilalt, south-eastern Morocco. The thickness of the different units is variable over the region, as are details of the stratigraphy. Approximately 45 m of the Ifezouane Formation is seen at Al Gualb, with perhaps as much as 20 m not exposed at the base. The Aoufous Formation is approximately 40 m thick at this location, and the full sequence is exposed. Only the lowest few metres (~8 m) of the Akrabou Formation are present at the top of the succession.

Approximately 45 km north of this locality the Cretaceous strata are caught up in the Atlas Mountain fold belt, but they still yield teeth and bones typical of the Tafilalt assemblage. Beyond the Tafilalt to the south and south west, the Kem Kem beds crop out along the north-western margin of the Hamada du Kem Kem, paralleling the Moroccan/Algerian border region as far as Tagounite.

At the time of deposition, this part of Morocco was located on the southern margin of the Tethys Ocean at approximately 15–20 degrees north of the equator. It was characterised by an extensive fluvial plain dominated by northward flowing rivers draining the continental interior and terminating in broad deltaic systems on Tethys' southern shores. The entire region was flooded by the early Cenomanian marine transgression that introduced carbonate deposition to a succession that had been dominated by siliciclastics from (probably) Late Jurassic times.

Across the Tafilalt and extending as far as Zguilma in the south-west and to Tadighoust in the north, the Kem Kem beds are divided into two units. The lower unit, the Ifezouane Formation, is characterised mainly by fine to medium sandstones, often of a dark brown colour, and forming tabular outcrops. The upper part of the Kem Kem beds, identified as the Aoufous Formation, is

dominated by fine, muddy sandstones at its base, passing quickly up into variegated mudstones with thin siltstones. The boundary between these two formations is ill-defined and needs re-evaluating.

Aferdou Zrigat: At the *Spinosaurus* dig site a sedimentary sequence commencing in the lower parts of the Kem Kem beds is exposed intermittently along a wadi and on the flanks of the escarpment of the Ikhf n Taqmout mesa. A detailed measured section on a better exposed and more continuous sequence of a neighbouring slope was reported by Ibrahim et al.[7]. The underlying basement and basal units of the Kem Kem beds can be accessed just a couple of kilometres to the south of the dig site. The lowest beds exposed comprise a sequence of fine sands and silts of grey, brown, pink and reddish hues. Typically, they display planar and cross bedding. There are thin hiatuses and event horizons that yield fossils of typical Kem Kem vertebrates including scales of lepidotid fishes, rostral teeth of the sawfish *Onchopristis numidus* and teeth of the theropod dinosaurs *Spinosaurus* and *Carcharodontosaurus*. Commercial diggers operate just two kilometres from the *Spinosaurus* dig site, where they excavate fossils from thin conglomeratic event horizons in the upper parts of the Ifezouane Formation. The passage from the dominantly sandy facies of the Ifezouane Formation into the silty mudstones and mudstones of the Aoufous Formation is transitional, and difficult to pinpoint: the *Spinosaurus* site lies at this transition.

The matrix in which the bones of FSAC-KK 11888 are preserved is variably fine sand, silt and clay. The sediments exhibit brown, red, yellow, purple, green, grey, and white hues. Millimetric-scale lamination is sometimes present, and often convoluted, suggestive of ‘dinoturbation’ or wet sediment deformation, although neither flame-structures nor ball and pillow structures have been observed at the site. Bivalves were occasionally encountered during the excavation and preserved as internal moulds of articulated individuals, resembling heterodonts (clams), but distinct from freshwater unionids. Above the dig site, the strata pass up into gently

dipping silty mudstones, likely deposited on a muddy pointbar of a meandering river. A map of all bones figured in situ (Extended Data Figure 3) shows a random distribution, with only three pairs of vertebrae lying in articulation. In addition, there is no evidence for preferential dispersal by water currents. Vertebral centra and lighter elements, such as neural spines and chevrons, appear scattered in all directions, and simply oriented/deposited by gravity in the most stable position, according to their shape.

2. Description of new material of the neotype of *Spinosaurus aegyptiacus* (FSAC-KK 11888)

In addition to previously reported elements[7], the neotype specimen now also includes new fragments of the cranium and mandibles, several previously missing bones of the left and right pes and, most importantly, most of the caudal vertebrae, which are the subject of the description in this paper (Figure 1, Figure 2, Extended Data Figure 3, Extended Data Figure 4). The new finds include many elements that perfectly match counterpart fragments of the hind limbs, the most complete dorsal neural spines, and other finds collected in the initial excavation in 2008. In addition to two fragments of neural arch belonging to one of the first caudal vertebral centra, unequivocal evidence that these elements pertain to a single *Spinosaurus* skeleton is provided by two key finds (Extended Data Figure 5): 1) a right astragalus, unearthed in situ in July 2019, that perfectly fits a corresponding notch on the distal end of the right tibia, excavated by the local collector in 2008; 2) fragments collected from the site debris during the 2015–2018 expeditions connect a (formerly indeterminate) shaft to the base of a dorsal neural spine, also excavated in 2008. This is confirmed by the perfect matching of the fractures and the unique combination of colours (black-white-brown-red) seen in cross-sectional view. For additional information, see also Part 3 below.

The caudal material represents the most complete tail yet recovered for a spinosaurid dinosaur, and one of the most complete for any basal tetanuran. In FSAC-KK 11888, more than 30

near-sequential caudal vertebrae are preserved, representing 4/5th of the tail of the animal and ranging from the proximal to the distal region. The caudals can be confidently placed in a sequence, from Ca1 to Ca41, based on both size and shape criteria as well as the original association of remains. Using the same criteria, even fragmentary remains can, in most cases, be placed accurately. Many bones exhibit slight to moderate postmortem damage and diagenetic deformation. This affects not only the slender neural spines (which frequently have multiple cracks), but also several centra (Extended Data Figure 1, 2, and 4). The mode of deformation is consistent with the undulating bedding plane of the fossiliferous layer observed in situ. There are no obvious traces of injuries or pathological conditions.

A total of 29 centra have been recovered to date, and most are well preserved. Positions 5, 6, 17, 36, and 38–40 are missing; 1, 3, 7, 18, 30, and 35 are represented by fragments. The position represented by a natural (syndiagenetic) clay mould (Figure 1, Extended Data Figure 4) is uncertain. Approximately the same number of neural arches is represented, although some of them consist only of neural spine fragments. In addition, 19 more or less complete haemal arches (chevrons) have been recovered from the site.

Without taking into account the cartilaginous joints/intervertebral discs, the preserved tail is approximately 400 cm long. Based on comparison with other theropods, we estimate a total tail length of approximately 530 cm, and a total caudal count of around 50. This estimate is consistent with a previous length estimate[7] for FSAC-KK 11888. It suggests that, at present, about 15 of the distalmost elements appear to be missing. By comparison, there are ~40 caudals in coelophysoids, 47 in *Dilophosaurus*, 50 in *Ceratosaurus*, and 50–60 in basal tetanurans[1].

The transition point is located at the level of Ca19 (the last vertebra bearing transverse processes), approximately halfway along the tail, at about 217 cm from the tail base. By comparison, the transition point is at Ca27 in *Allosaurus* and around Ca15 in most coelurosaurs[1].

This point marks, approximately, the distal termination of *m. caudofemoralis longus*, and the point at which the *m. ilio-ischiocaudalis* begins to insert across the entire lateral surfaces of the haemal arches and centra, instead of having dorsal insertion points on the transverse processes[48]. At the transition point, the prezygapophyses cease any overlap with the preceding centrum and show a conspicuous decrease in size. The postzygapophyses also decrease in size, reflecting a reduced degree of contact with the prezygapophyses via the joint capsule and accessory ligaments. This condition is distinct from the trend observed in most theropods, wherein the zygapophyses become increasingly elongate and important in their articular function towards the distal end of the tail[1]. Overall, in *Spinosaurus*, the zygapophyses are significantly less developed than in most tetanurans, hinting at a different functional capacity for the tail in this taxon. Vertebrae in the proximity of the transition point are also distinguished by a change in the shape of the centra (more elongate) and in the size of the base of the neural arch (shorter and smaller).

Unfortunately, the neural spines of the first three caudal vertebrae are not preserved. Our reconstruction predicts that they would have been shorter than the spine of Ca4, this being the point of maximum dorsoventral flexion of the tail. In this respect, we argue again for the referral to *Spinosaurus* of a caudal vertebra described by Stromer[12]. This was questioned by various authors in the past[49,50], but based on comparisons with the new material described here we confirm its attribution to *Spinosaurus* and the validity of the association of Stromer's holotype, and we propose that the vertebra in question is most likely to be caudal 2 or 3 (Extended Data Figure 6).

At the level of Ca4, the bony core of the tail is wide; about 50 cm across the transverse processes, with a dorsoventral height of 51 cm without the chevron (as preserved - the tip of the spine is missing), and about 70 cm including this element. These proportions clearly indicate that the basal portion of the tail was relatively expanded (both transversely broad and dorsoventrally

deep). At the level of Ca7, the neural spine is incomplete. The estimated dorsoventral depth is about 80 cm, whereas the transverse breadth is smaller, at about 40 cm.

At Ca23, the centrum is smaller, but the neural spine is much more elongate. However, as the neural spines, from Ca11–12 onwards, are inclined distally at an angle of 45°, the dorsoventral depth of the distal portion of the tail is similar to that of the proximo-medial portion - about 70 cm. The chevrons in this region of the tail are as elongate, or even slightly more elongate than those for more proximal caudals. Conversely, the transverse diameter of the tail is much narrower, with centrum 23 being only seven cm in breadth. At the level of Ca31, the dorsoventral depth of the tail appears to have been slightly lower because the spine shows greater recurvature, bending to the right (although this is likely due to diagenetic deformation). The transverse breadth of the centrum is six cm. At the level of Ca36, the centrum is smaller, with a transverse breadth of four cm and the dorsoventral depth of the tail is slightly lower because the neural spine forms 90% the length of the spine of Ca31, indicating a trend in height reduction towards the distal end of the tail, which is confirmed by Ca41: it represents the distalmost preserved vertebra, with a neural spine that is 72% the length of the Ca31 spine.

The best preserved among the first 16 caudal vertebrae of FSAC-KK 11888 do not have neural arches that are fully fused to the centra (the neurocentral suture is still visible or at least only partially obliterated). Only fragments of Ca17 and Ca18 have been recovered; from Ca19 onwards, sutural fusion is complete.

Centra: The vertebral column of *Spinosaurus* is characterised by amphicoelous caudal vertebrae. In Ca7, the deepest point in the centre of the concave proximal face is three cm below the rounded rim of the face. All other elements show only a minor degree of amphicoely.

The articular faces are round, or nearly so, with the maximum transverse breadth located slightly ventral to mid-height. Facets for the haemal arches are prominent throughout the entire vertebral series, with the ventral border of the distal articular face of the centrum bearing ventrodistally directed articular surfaces.

Although the centra are hollow (as seen through several broken surfaces), there is no evidence of foramina to suggest that the caudal vertebral series was pneumatised. Small openings are variably present on the lateral surfaces of the centrum of Ca1. Similar openings are visible also in the sacrals and are probably vascular/neurovascular in nature. The lateral surfaces of the centra, however, bear oval fossae (dorsolateral fossae as in *Ceratosaurus*[51]) just ventral to the neurocentral suture. This emphasises the transverse constriction of the centra, especially in the distal half of the preserved part of the tail, where the centra are relatively longer.

From Ca10 (Ca14 of 7) onward, the ventral surface of the centrum bears a longitudinal groove (as in many non-tetanuran neotheropods, such as *Dilophosaurus*, coelophysoids, and *Ceratosaurus*[51]).

The articular faces of Ca1 correspond closely to the transition in size between S5 (smaller diameters) and Ca2 (larger diameters). According to the position of the fifth sacral vertebra and the size of the ilium, the first caudal vertebra was positioned distal to the postacetabular blades of the ilia.

Both in absolute size and proportions, the caudal centra are shorter than the dorsal centra: the longest caudal centrum (Ca15) is 120 mm long. By contrast the mid-dorsals (D6–D8) are 170–180 mm long (Extended Data Table 1). In the tail of FSAC-KK 11888, the centrum length reaches approximately twice the centrum depth in only the distalmost preserved vertebrae. The diameter of the centra decreases in more distal positions, but the overall proportions of the centra remain nearly the same.

Neural arches: The neural arches represent the most characteristic elements in the tail of *Spinosaurus*. A complex of vertebral laminae and fossae is present in arches of the proximal caudal vertebrae and partly persists distally to the mid-caudal neural arches. Ca4 provides the best example, so this is used as reference for anatomical nomenclature, which follows[52,53,54]. The major vertebral processes of the neural arch (neural spine, zygapophyses, transverse processes) are buttressed by robust laminae that project in all three spatial planes with a triradiate or even a multiple radiating pattern. Between these laminae, a number of fossae ensure that the structure remains lightweight (see list of laminae and fossae below). *Spinosaurus* is unique among theropod dinosaurs in that the spinodiapophyseal laminae are the most developed laminae, starting from Ca11. They are the only spinal laminae present from Ca19 to Ca31 (although irregularly expressed, see below).

The anterior centrodiapophyseal lamina (acdl, extending from the proximodorsal corner of the centrum to the transverse process) and the posterior centrodiapophyseal lamina (pcdl, extending from the transverse process to the distodorsal corner of the centrum) are well-developed, bounding fossae that become shallower throughout the sequence and that are almost lost by Ca11.

The proximal prezygapophyseal processes have a lateral strut corresponding to the prezygodiapophyseal lamina (prdl) that extends to the transverse process. A spinoprezygapophyseal lamina (sprl) is also present, connecting the distodorsal margin of the prezygapophysis to the proximal surface of the neural spine. The spinopostzygapophyseal lamina (spol) extending from the lateral margin of the postzygapophysis to the distal surface of the neural spine is clearly visible on caudals up to the transition point (e.g., Ca10). From here on, the postzygapophyses are increasingly reduced and the spinopostzygapophyseal laminae tend to migrate into the medial sagittal plane,

becoming indistinguishable from the postspinal lamina (posl). Other spinal laminae associated with the neural spine are described below and illustrated in Figure 2.

In caudals up to the transition point in the tail (Ca19) the prezygapophyseal processes extend proximodorsally past the proximal limit of the centrum, while the postzygapophyses of caudals up to and including Ca21 extend past the distal limit of the centrum. In this transitional region of the tail the zygapophyseal facets decrease in size.

In the most proximal caudals (Ca4), the zygapophyseal facets are well-developed and angled at about 150° to the vertical plane. In Ca12, this angle increases to 165° and the flat suboval facets are slightly reduced. Beginning from Ca16, less than 30 cm before the transition point, the zygapophyseal facets become almost vertical, paralleling a plane that is only 10–20° from the dorsoventral axis of the vertebrae (prz, dorsomedially; poz, ventrolaterally), facilitating transverse excursions of the tail. This interpretation is consistent with the absence of accessory hyposphene-hypantrum articulations, and the short zygapophyses in which articular contact was reduced, especially in the portion of the tail distal to the transition point. Dorsoventral mobility and ventral flexibility of the tail were limited dorsally by the presence of the very long neural spines.

In Ca4 the neural arch articulates with the centrum along its entire length, and shows only a slight distal inclination. In proximal caudal vertebrae the neural spines reflect the orientation of the base of the arches and are also slightly recurved, overhanging the distal face of their centra. Distally from Ca7, the neural arch becomes more inclined, so that the base of the neural spine is positioned dorsal to the distal half of the centrum and the neural spine overhangs the succeeding centrum. From Ca11–12 on, throughout the caudal series, the neural spine becomes more inclined at the base, maintaining a remarkably constant angle of 45°. This orientation, coupled with the extreme length of the spine, means that the tip of the spine overlaps a point more than three centra distal to the

vertebra from which it originates, aligning with the proximal face of the fourth succeeding vertebra (Figure 1, Extended Data Figure 4).

The morphology of the neural spine varies along the tail. The base of the neural spine of proximal caudals is cruciform in cross-section. This reflects the presence of two prominent spinodiapophyseal laminae, together with the prespinal (prsl) and postspinal lamina (posl), which served as attachment sites for the interspinous ligaments[52]. These ligaments were likely well-developed, given that the prespinal lamina forms a prominent median buttress. The buttress extends proximally reaching the level of the prezygapophyses through an extraordinarily thin "webbed" process (see Ca11–12). Distal to the transition point, however, the prespinal lamina is only very weakly expressed and then disappears, while the postspinal lamina is reduced to a keel. Consequently, the spines become triangular in cross-section.

By contrast, the spinodiapophyseal laminae are not reduced: beginning with Ca15, the neural spines of *Spinosaurus* are strongly expanded transversely (a unique feature among theropods). This expansion is contributed to both by the body of the neural arch/spine, and by lateral expansions of the spinodiapophyseal laminae, which are most evident in Ca16, but variably expressed (due to diagenetic deformation) in Ca19, 21, 22, and 29. The supporting axis of this unique structure consists of two rods (distal projections of the arms of the neural arch) united by a flattened central portion. Ca16 also exhibits a deep, strongly developed postzygapophyseal spinodiapophyseal fossa that displaces and almost isolates the postzygapophyses in a more distal position. This fossa and the postzygapophyses become reduced in the following caudals, almost disappearing by Ca23, which has only vestigial postzygapophyses. Distal to the postzygapophyses, the two rods of the neural spine begin to taper and fuse in the midline, creating a U-shaped cross-section with the concavity facing proximally. This is found in most distal caudals and is easily recognizable even in fragmentary spines (e.g., Ca30). The concavity terminates at the apex of the

basal third of the spine, where the two rods become a single rod, elliptical to oval in cross-section (see Figure 1, Supplementary Movie S02). The latter becomes rounded at the beginning of its distal third, then becomes transversely elliptical again. The neural spine of Ca23 terminates in a flat surface, taking the form of an apical expansion characterised by a rugose surface texture. This apical expansion is present from Ca15 to Ca36, and is more marked in distal caudals. It probably served as a location for supraspinal ligament attachments[55]. This complex morphology helps to identify even the smallest fragments of spine recovered.

The morphology of the base of the neural spine, with the two rods connected by a flattened central portion, is comparable to one of the two caudal vertebrae of "*Spinosaurus* B" figured by Stromer[56] (Tafel I, figs. 6a–c). The centrum morphology is also similar, emphasising the close comparability of the Egyptian and Moroccan specimens. Based on the caudal series of the neotype, the position of the element figured by Stromer is likely to lie between Ca20 to Ca25. In the vertebrae that are less distorted, the neural canal is rounded in outline and between 10 to 22 mm in diameter.

The transverse processes originate at the base of the neural arch, and are closer to the neurocentral suture in the mid-caudals. They are horizontal or exhibit a slight dorsal elevation (circa 10° above the horizontal in Ca11). In dorsal view, the transverse processes are almost perpendicular to the centrum or slightly distally inclined (circa 10° from the perpendicular in Ca12), but never overlap the caudal margin of the centrum. The lateral portion of the transverse process slightly expands proximodistally, prior to the end of the process.

The length of the transverse process reaches a maximum on proximal caudal vertebrae, where it greatly exceeds centrum breadth (in Ca4 the transverse process is almost two times longer than the transverse diameter of the faces of the centrum; see Extended Data Table 1). The transverse processes gradually decrease in size along the caudal sequence (the transverse process is as long as

the centrum breadth in Ca11), up to the transition point, after which they are entirely absent. Based on the shape of the centrum and the development of the transverse process, the caudal vertebra figured by Stromer[56] (tafel I, fig. 5a, b) closely matches Ca11 of FSAC-KK 11888.

Haemal arches: Nineteen haemal arches (chevrons) are preserved for the tail of FSAC-KK 11888, although some of them are incomplete (Figure 2, Extended Data Figure 4, Extended Data Table 2). The most distinctive feature of the chevrons of *Spinosaurus* is that their morphology shows little variation throughout the preserved portion of the caudal series. Except for a small and gradual reduction of the haemal canal, distal chevrons are as elongate as those located more proximally, though they do become more slender, paralleling the gradual decrease in size of the centra. It cannot be excluded that the terminal quarter of the tail had smaller chevrons with a ventral half that angled distally and expanded dorsoventrally. However, the morphology of the preserved portion of the tail, extending far beyond the transition point, is highly conservative, ensuring a constant depth for the ribbon-like tail, a remarkable feature that, as we show here, is likely related to aquatic locomotion.

Each haemal arch is sling-shaped in proximal and distal views. The two arms have expanded proximal heads (especially mediolaterally), and are transversely flattened to cylindrical in their proximal halves. The distal half of the chevron is transversely compressed with a lamina connecting the two arms, and the distal termination is slightly expanded, with tendon attachment scars.

Rather than two distinct articular facets, each head of all preserved chevrons bears a single dorsally convex articular surface directed proximodorsally. These facets match the size and position of concave articular facets situated on the ventrodistal edge of the centrum. Consequently, each chevron mainly articulates with the more proximal centrum of the vertebral pair, although contact with the distal member was likely present.

The haemal canals are oval in outline, the greatest diameter being dorsoventral. From the base of the tail to the transition point (Ca12), the canal occupies about half of the chevron height. In the mid-distal caudals (Ca24–32), the canal is reduced to one-third of the haemal arch. Consequently, the dorsoventral diameter of the haemal canals ranges between 65 and 53 mm. The transverse diameter becomes gradually smaller, matching the decrease in size and width of the related centra. The haemal canals are generally open dorsally, although in three cases the medial expansions of the heads contact each other, closing the canal.

Tail muscle reconstruction (additional comments on Figure 1): Dissections of extant vertebrates and study of prepared specimens by CDS, NI and SM, as well as recent comparative studies[48] were used to generate the reconstructed tail cross-sections shown in Figure 1. We adopted a highly conservative approach to tail reconstruction[57] incorporating a minimum number of muscles and a minimum volume and mass for each. Consequently, the swimming performance values generated by the mechanical analyses likely also represent a minimum for this tail type. It is possible that the tail bore a larger muscle mass than that shown in our reconstruction and may have had its surface area further extended by integumentary structures (e.g., tall scales or a fin), in which case the forces generated were likely larger than those proposed here.

In our reconstruction the ventral part of the tail of *Spinosaurus* accommodates more muscle than the dorsal portion, and is thus deeper and more massive along its entire length. Unique among the caudal muscles, the *m. caudofemoralis* is not partitioned by conical myosepta, and its overall form more closely resembles a limb muscle rather than an axial muscle. This is based on the same circumstances among extant reptiles[48] and has also been reported for nonavian theropod dinosaurs, where elongate parallel fascicula (bundles) of myofibres have been directly observed in the exceptionally preserved *m. caudofemoralis* of *Scipionyx*[58]. Distal to the transition point, the *m.*

caudofemoralis longus is gradually replaced by the *m. ilio-ischiocaudalis*, which becomes the principal caudal muscle in this region of the tail. The *m. ilio-ischiocaudalis* is composed of conical myomeres which, on the muscle surface, are depicted as divided by rhomboidal interlocking zigzag septa. This parallels the occurrence of this structure in extant and extinct[48] taxa. Where the *m. caudofemoralis* terminates, the *m. ilio-ischiocaudalis* then inserts across the entire lateral surface of the centrum and haemal arch. As the haemal arches are unreduced and proportionally very deep it seems likely that this muscle was, concomitantly, deep and bulky in *Spinosaurus*. The short conical myomeres, which articulated via vertical zigzag septa, were well suited for generating lateral undulation. Extant crocodilians rely entirely on this muscle when swimming with the distal end of the tail[59].

By contrast, it seems likely that only the basal third of the neural spines was enclosed by the *m. spinalis* and *m. longissimus*. The main bulk of these muscles likely occurred in the proximal portion of the tail as the neural arches of middle and distal caudals are quite low and only the neural spines are elongate. The dorsal terminations of the distal neural spines in *Spinosaurus* are enlarged, but this most probably represents attachment sites for the supraspinal ligament rather than muscles[55].

3. Evidence in support of the interpretation of FSAC-KK 11888 as a single individual

Two separate lines of evidence support the argument that the skeletal remains recovered from Aferdou Zrigat represent a single individual.

Anatomical and taphonomic evidence:

- No duplicates of paired bones have been recovered;
- There is no overlap of any skeletal elements;
- All contralateral elements are symmetrical in shape and size;

- Anatomically adjacent bones articulate perfectly;
- The bones were collected from a single, well-defined horizon and the distance between bones generally does not exceed more than two metres;
- All the bones were covered in a highly atypical sedimentary matrix[7];
- There is no taphonomic evidence for sorting or selection of skeletal elements;
- The peculiar proportions (appendicular skeleton vs axial skeleton) of FSAC-KK 11888 are consistent with those of Stromer's *Spinosaurus* B; the pes is not comparatively small and it is undoubtedly associated with the other parts of the hind limbs, further evidence that the relative shortness of the femur and tibia is a peculiar feature;
- Associated dinosaur skeletons are exceptionally rare in the Kem Kem beds, with FSAC-KK 11888 representing the first discovery of associated cranial and postcranial dinosaur remains after almost 70 years of palaeontological work in the region.

Osteohistological evidence: Histological details of the femur of FSAC-KK 11888 were figured by Ibrahim et al.[7]. The fibula has an oval cross-section and is solid, lacking a medullary cavity. The microstructure consists of woven-fibrolamellar bone. The vascularisation is mainly longitudinal and tends to decrease in density towards the surface of the bone, though still present in the outer-most zones. Haversian systems are abundant in the inner cortex and extend to the surface of the bone in the left area of the bone thin section. Ten LAGs are present in the fibula, and retrocalculation suggests that a further five can be added to this total. The spacing between the LAGs decreases towards the surface of the bone. An External Fundamental System (EFS) is absent.

The cross-section of the rib is triangular. The rib is dense, with trabeculae invading a small medullary cavity and defining a gradual transition between the medullary cavity and the compact bone. The microstructure consists of woven-fibrolamellar bone. The vascularisation is mainly

longitudinal and is rarer in the outer cortex. Haversian systems are very dense in the inner cortex, with at least four generations present, but are absent in the outer-most part of the rib. Six LAGs were counted in the rib and, using retrocalculation, a further 10–11 LAGs can be added to this total. An external fundamental system (EFS) is absent, with rarefied primary vascularisation still present in the outer cortex.

Thin sections of the neural spine vary between oval (basally) and semi-rectangular (distally) in cross-section, depending on the height at which the section was made. The medullary bone is highly reduced, especially in comparison to other sail-backed dinosaurs, such as *Ouranosaurus nigeriensis*[33]. The microstructure consists of woven-fibrolamellar bone. The vascularisation is longitudinal and shows a decreasing trend in density towards the external surface of the bone. Haversian systems are present in the inner compacta, but absent in the outer cortex. Approximately five to six LAGs can be identified in the primary bone and six missing LAGs can be inferred. The spacing between LAGs decreases towards the surface of the bone. An EFS is absent in both the neural spines examined.

The same ontogenetic pattern is common to all of the examined skeletal elements: 1) the vascularisation and the spacing between LAGs tends to decrease towards the external surface; 2) vascularisation is still present in the outer-most compact cortex; 3) Haversian systems are abundant in the inner compact cortex, but rare or absent in the outer cortex; 4) an EFS is absent in all bones sectioned. A sub-adult ontogenetic stage is inferred for all of the bones investigated. This interpretation is based on the density of vascularisation and its decrease through the compact cortex, the presence of remodeling in the inner cortex, the decreasing in spacing between the LAGs, and the absence of an EFS. Differences in the number of LAGs in skeletal elements have been discussed in the literature and interpreted as evidence for different allometric trajectories, growth rates, rate of remodeling and cortical compactness of the skeletal elements[60,61,62,63,64,65,66]. However, ontogenetic

patterns can be observed and compared in the microstructure of all the skeletal elements, in particular reduced spacing between LAGs and the presence of remodeling[63].

The long bones and the rib show a comparable number of LAGs. By contrast, the neural spine shows considerably fewer LAGs. This is likely related to the peripheral location from which the sample was taken. Because neural spines grew increasingly tall during the life of the individual, the most complete record of growth is expected in the basal portion of the neural spine, as observed in other taxa such as *Ouranosaurus nigeriensis*[33]. However, even if histological details evident in the apical portion of the neural spine do not provide the best approximation of the absolute age of the individual, the growth record pattern certainly confirms the ontogenetic stage.

In addition to the details reported above, all bones have a reduced medullary cavity with a dense and compact cortex, a character that is seemingly exceptionally rare in non-avian theropods[7]. In the fibula the medullary cavity is absent, while spongiosa-like microstructure is present in the innermost cortex of the femur, the rib, and the neural spine. The tibia of *Spinosaurus* was also examined thanks to a deep crack in the midshaft of the bone. It too lacks an open medullary cavity, sharing with the femur and the rib a spongiosa-like structure within the inner cortex.

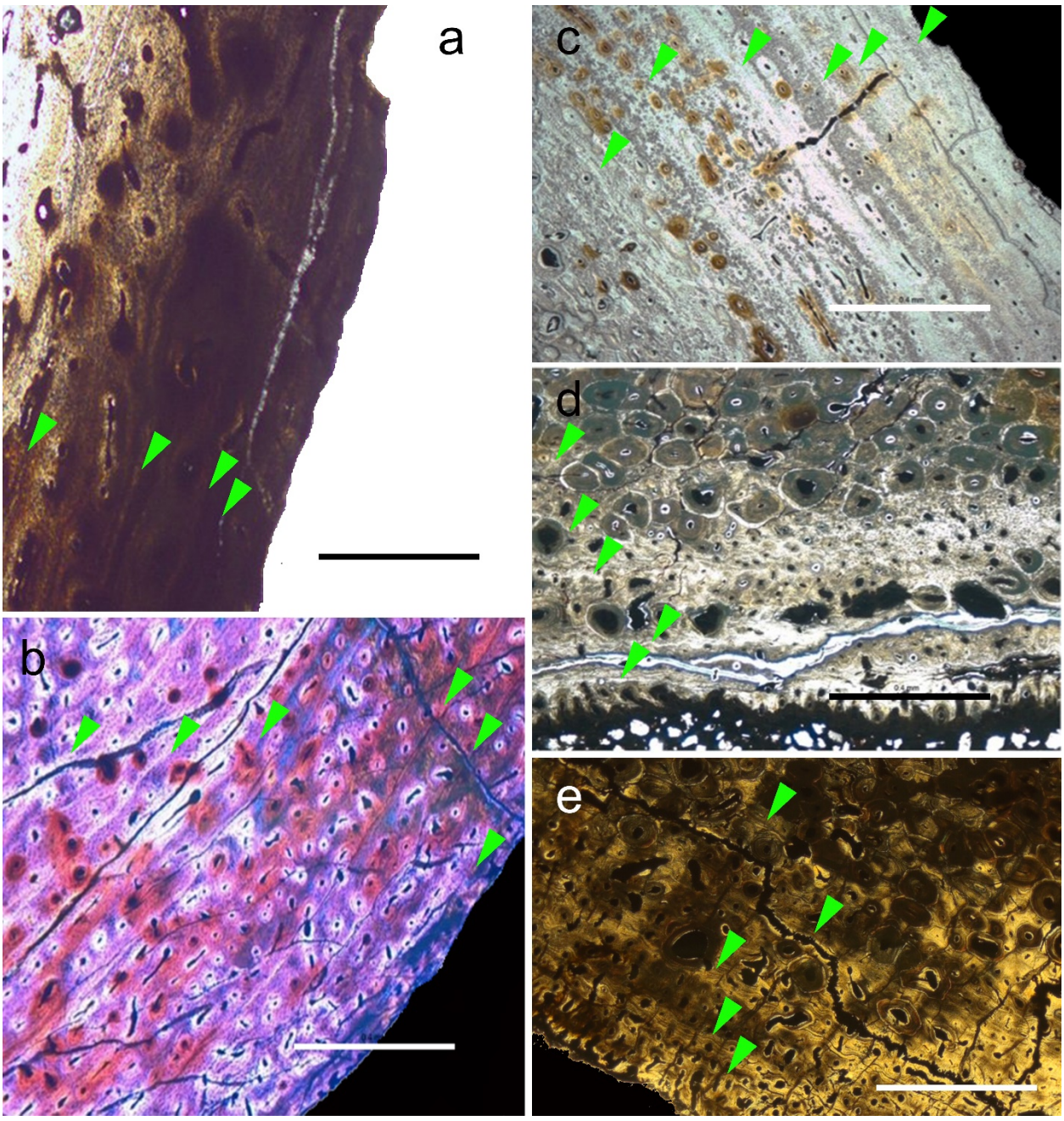

Supplementary Information Figure S2. Osteo-histology of the five skeletal elements assigned to the neotype (FSAC-KK 11888) of *Spinosaurus*. a) Close up of the outer cortex of the diaphysis of the femur; b) outer cortex of the fibula in crossed nicols; c) details of the outer cortex of the dorsal rib; d–e) outer compacta of the neural spines. Green arrows indicate LAGs. Scale bar equals 0.5mm in (a) and 1 mm in (b–e).

4. Referral of FSAC-KK 11888 to *Spinosaurus aegyptiacus*.

The referral of the new specimen to *Spinosaurus aegyptiacus* and its designation as a neotype was questioned[9] on anatomical and taphonomic grounds and because of concerns about the geographical location of the neotype. The new material includes caudal elements that can be directly matched to those described by Stromer (Extended Data Figure 6), in addition to previously published comparisons[7]. In addition, some elements from our recent excavations can be matched to the first bones excavated at the site by the local discoverer (Extended Data Figure 5).

Evers et al.[9] questioned both the association of FSAC-KK 11888 and the association of Stromer's specimens. Similarities between the vertebrae of *Sigilmassasaurus* and Stromer's *Spinosaurus* B were not considered strong enough to support conspecific or, at least, congeneric status. Our new finds unequivocally demonstrate the genuine association of FSAC-KK 11888 and strongly support the idea that the remains described by Stromer were also associated. In light of the well-known difficulties in defining a species in palaeontology, we pragmatically refer material to one morphologically variable species, *Spinosaurus aegyptiacus*, rather than to multiple closely-related spinosaurines sharing unusual proportions and characteristics, such as small hind limbs and extremely elongate neural spines. We follow Ibrahim et al.[7] in considering FSAC-KK 11888 as the neotype, which is now the most complete theropod skeleton from the Cretaceous of mainland Africa, far surpassing the holotype in completeness.

Lastly, there is little justification for the taxonomic separation of Egyptian and Moroccan material on the basis of geographical location[9] when considering, for example, the distribution of extant taxa, such as *Crocodylus niloticus*[67] and *Panthera leo*[68].

5. Photogrammetry

We scanned eight of the new caudal vertebrae and two of the chevrons recovered during the 2018–2019 excavations. The material scanned includes Ca4, Ca7, Ca12, Ca16, Ca23, Ca24, Ca31, and Ca41 and the chevrons Chv7 and Chv24 (Supplementary Information Movie S02). In addition, we scanned the newly found astragalus and re-scanned all the other bones of the pes of FSAC-KK 11888.

To perform photogrammetry and obtain the 3D models we used a Nikon D7500 with a 50 mm lens, following the classic method that comprises these phases: shooting, masking the photos, aligning photos, building a point cloud, building the mesh, texturing the mesh, and post-production of the 3D model obtained. See Mallison & Wings[69] for a detailed description of the photogrammetry workflow.

The following rules were adopted. We did not use flash photography; all photographs were shot in manual mode; a small aperture (f13 to f18) was used to obtain a suitable depth of field; the ISO was set at the lowest value possible, removing some of the noise from the photos; a high shutter speed was used to avoid blurring; for the same reason, a tripod and a touch screen display proved essential. Two approaches were used:

1. Small specimens. These were scanned in a lightbox (Supplementary Information Figure S3). A lightbox gives best results for photogrammetry as it provides optimal and perfectly diffuse light. This allows the photographer to shoot with the ISO set at the lowest value possible, while still using a small shutter speed and small aperture. The dimensions of the lightbox are the only limitation. With a lightbox, the camera remains in the same position, while the specimen is moved and turned around in order to scan every aspect of the fossil ("turntable method").

2. Large specimens. As these would not fit in a light box, two alternative experimental approaches were used. A) Sunlight/natural light conditions or a few spot lights were used to

illuminate the specimen; a direct light source requires circumnavigation of the specimen ("walk-around method"); in this case, the turntable method is unsatisfactory as the light conditions change for each photograph and the software is unable to correctly align the photos. B) Low light conditions, typically in a room without or with a low direct light source, are preferable since the light, although low, is still diffuse. In such an environment it is possible to "mix" the turntable and the turn-around method to produce good quality results, although the ISO must be set relatively high and consequently shutter speeds must be low.

Supplementary Information Figure S3. Right 3rd ungual of FSAC-KK 11888 (resin replica) ready to be scanned.

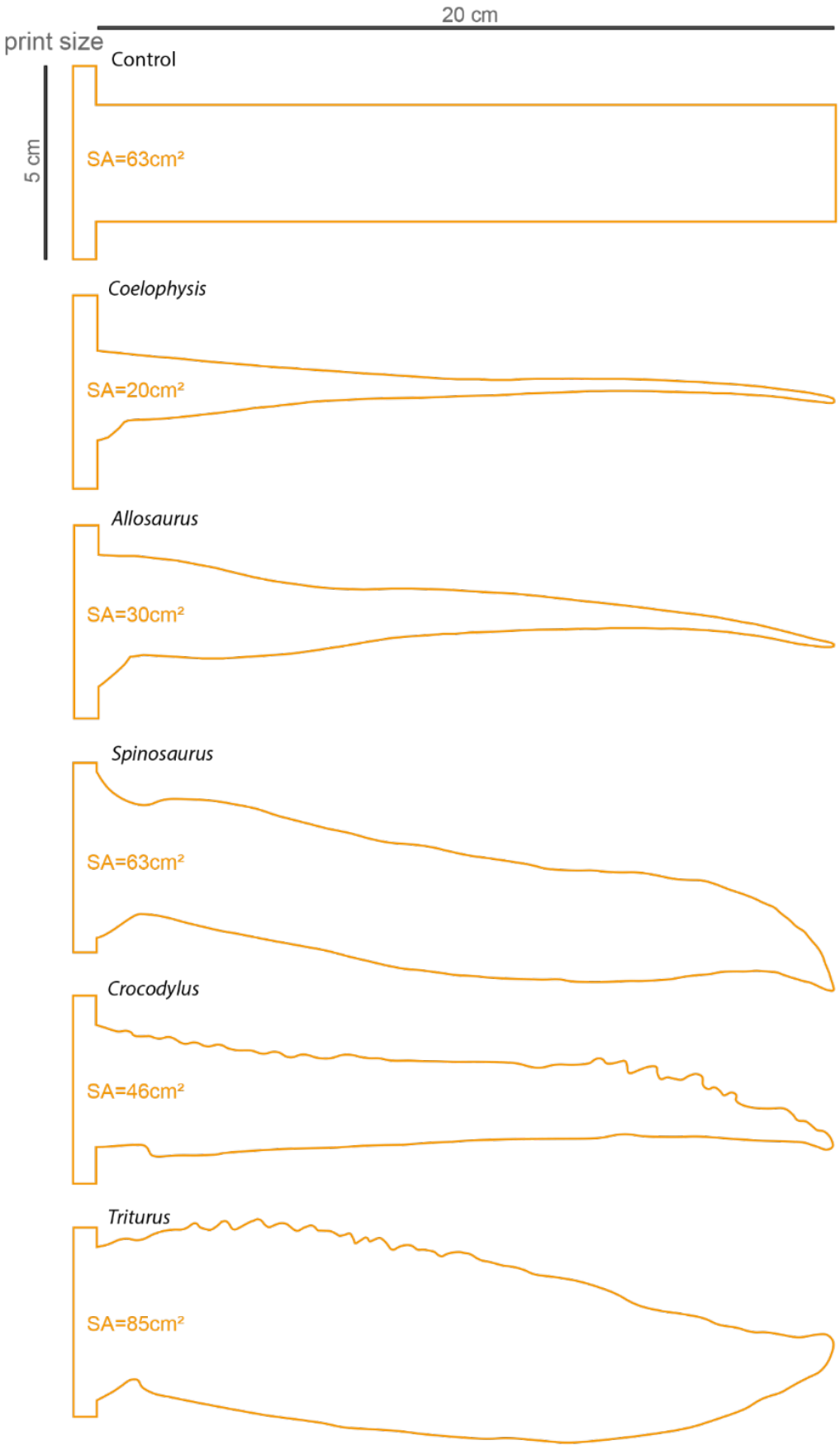
20 cm
print size
5 cm
Control
SA=63cm²
Coelophysis
SA=20cm²
Allosaurus
SA=30cm²
Spinosaurus
SA=63cm²
Crocodylus
SA=46cm²
Triturus
SA=85cm²

Supplementary Information Figure S4. The six different tail shapes (and corresponding surface areas) used in experimental testing of swimming performance (see Methods in main article). The tail shapes were manufactured from 0.93 mm thick plastic of flexural stiffness $5.8 * 10^{-5}$ Nm^2 and were cut using an Epilog Zing24 laser cutter.

6. Whole-body reconstruction

A full body flesh reconstruction of *Spinosaurus* (Extended Data Figure 7) was digitally built by one of us (DB), using the Claytools 3D modelling software. It is based on the new skeletal restoration (bones and other hard tissues, and a silhouette of the soft tissues) presented in Fig. 1, which, in turn, is largely based on specimen FSAC-KK 11888. This specimen shows the following combination of unusual features: long and low jaws with conical teeth; nasal crest; long dorsal vertebrae with extremely tall neural spines; small ilia; hind limbs with short stylopodium and zeugopodium, and, at the same time, wide pes with enlarged digit I and large, flat pedal unguals; and a remarkable ribbon-like, dorsoventrally expanded tail. Skeletal elements not preserved in FSAC-KK 11888 are based on isolated remains referred to *Spinosaurus*[7,70], as well as on the most closely related spinosaurid species for which those features are known, following the methodology proposed by Bryant & Russell[71]. Although the taxonomy and biology of *Spinosaurus* are still controversial[9,14] we note that similar referrals in the case of other spinosaurids (e.g., *Irritator/Angaturama*) have not proven as controversial, even in the absence of a detailed geological context[20]. Similarly, remains of *Suchomimus* and *Baryonyx* have been used in composite reconstructions[20]. In the case of *Spinosaurus* this means that, even if two extremely similar spinosaurids inhabited North Africa in the Cretaceous (unlikely as this may currently seem), using these remains to reconstruct the anatomy of a giant, tall-sailed spinosaurid (*Spinosaurus aegyptiacus* according to Ibrahim et al., 2014a) would be well within the bounds of

standard practices for palaeontology and comparative anatomy.

The entire skeletal restoration was completed after having corrected for post-mortem, diagenetic deformations and linked all the known elements according to their morpho-functional interpretation. The restoration represents the most up to date summary of the knowledge of *Spinosaurus* skeletal anatomy, and emphasises its unusual body proportions and tail. The skeletal restoration was imported into ClayTools and superimposed on the model generated by Ibrahim et al.[7], allowing the modeler to update the anatomy of multiple areas (e.g., tail, pes, manus, dorsal muscles). An "in vivo" restoration, i.e., the full reconstruction of the living animal, scaled to match the same body size of FSAC-KK 11888, was generated in a symmetrical pose (Extended Data Figure 7a) for further estimates of body mass, segment masses, and whole-body center or mass. The restoration was also placed in a tail-propelled swimming position (Extended Data Figure 7b) for visualization purposes.

7. Body mass, segment masses, and centre of mass (CoM).

A volume of 3.864 m3 was calculated for our symmetric *Spinosaurus* model using the software MeshLab. To estimate body mass, we used a broad-range of body densities and % zero-density air cavities measured for extant aquatic archosaurs and non-avian dinosaurs (Supplementary Data File 2). For birds and crocodiles, Brassey & Sellers[72] reported the following homogenous density values: Anatidae (diving ducks) 990 kg/m^3; Spheniscidae (penguins) 1020 kg/m^3; Phalacrocoracidae (cormorants) 1030 kg/m^3; Gaviidae (loons) 1060 kg/m^3. A homogenous density of 1080 kg/m^3 was reported for *Crocodylus niloticus*[73]. A conservative homogenous density of 1000 kg/m^3 is often used in non-avian dinosaur body mass reconstructions[74,75,76,77], but zero-density air cavities in the head, neck, and torso are frequently taken into consideration. To account for zero-density air cavities, we applied six different density estimates: 1) mean homogenous density of 911.63 kg/m^3

given for the basal tetanuran *Acrocanthosaurus atokensis*[75]; 2) subtracted a mean zero-density air volume of 8.927% from the head, neck, and torso segment (calculated using 1000 kg/m^3) given for *Acrocanthosaurus atokensis*[75]; 3) subtracted a mean zero-density air volume of 8.312% from body mass (calculated using 1000 kg/m^3) calculated from all models presented by[75]; 4) variable segment densities (head density = 981.63 kg/m^3; neck density = 911.07 kg/m^3; torso density = 760.07 kg/m^3; all other segments density = 1000 kg/m^3) given for *Acrocanthosaurus atokensis*[75]; 5) mean homogeneous density of 833 kg/m^3 given for *Spinosaurus aegyptiacus*[10]; and 6) variable segment densities (head, neck, torso, hip density = 850 kg/m^3; sail density = 1200 kg/m^3; tail density = 1000 kg/m^3; limb density = 1050 kg/m^3) given for *Spinosaurus aegyptiacus*[10]. Using these values, we calculate a body mass range of 3,219-4,173 kg for an individual of *Spinosaurus* with the same body dimensions as FSAC-KK 11888 (Supplementary Data File 2).

In addition to estimating body mass, we also calculated the whole-body centre of mass (CoM) in Meshlab (Supplementary Data File 2). First, whole-body CoM was calculated using a homogenous body density of 1000 kg/m^3. We then took three approaches to incorporating zero-density air cavities into the head, neck, and torso segments and to consider variable densities of the sail and limbs. To do this, the symmetric model of *Spinosaurus* was cut in FlashPrint-4.1.0 into 10 segments: head, neck, torso, sail, left and right arm, left and right leg, hip, and tail. Segment masses and CoMs were then determined in Meshlab from a general coordinate system (+X = cranial; +Y = dorsal; +Z = left; units in meters) in which the tail tip was set to X = 0, Y = -1.29, Z = 0 and the snout tip to X = 10.37, Y = -0.81, Z = 0 (Extended Data Figure 8a). In the first zero-density calculation, the mean zero-density air volume of 8.927% given for *Acrocanthosaurus atokensis*[75] was distributed across the head (1.123%), neck (4.862%), and torso (94.003%). In the second zero-density calculation, variable segment densities were applied based on those given for *Acrocanthosaurus atokensis*[75]. Finally, in the third zero-density calculation, variable segment

densities were applied based on those given for *Spinosaurus aegyptiacus*[10]. This final analysis also considers the sail, hip, and limbs to have densities that vary from 1000 kg/m^3, thus taking into consideration a more extensive air sac system in the hip, reduced soft tissue in the sail, and reduced medullary cavities in the limb bones.

To calculate whole-body CoM, a custom Python script was written to implement the equations given by Bates et al.[75] for 3D model CoM estimation. Total body mass was calculated by summing the masses of all body segments minus the mass of the zero-density volumes as follows:

$$Total\ body\ mass = \sum Ms - Mzd$$

where Ms is the mass of the segment and Mzd is the mass of the zero-density volume in that segment using a density of 1000 kg/m^3. The CoM for the whole body was then calculated by multiplying the segment masses by the Cartesian coordinates of their centres of mass and dividing the sum of these by the total body mass:

$$Whole\ body\ CoM =$$

$$Xc = \left(\sum Xs(Ms - Mzd)\right)/Mt$$

$$Yc = \left(\sum Ys(Ms - Mzd)\right)/Mt$$

$$Zc = \left(\sum Zs(Ms - Mzd)\right)/Mt$$

where Xs, Ys, Zs are the Cartesian coordinates of the segments CoMs and Mt is the total body mass. All the relevant data to replicate our calculations are given in Supplementary Data File 2.

The resulting Cartesian coordinates of the four different whole-body CoM calculations are plotted on our *Spinosaurus* model in Extended Data Figure 8b and given in Supplementary Data File 2. From the cranial rim of the acetabulum measured cranially (in the +X direction), the CoM of *Spinosaurus* ranges between 0.725-0.825 m, which is more caudal than the 1.04 m calculated for our prior model[7] (Extended Data Figure 8d), but further cranial than the 0.48 m estimate given by Henderson[10] (Extended Data Figure 8c). Our results indicate that the expanded tail of *Spinosaurus* shifts the centre of mass of our "in vivo" model caudally, but not drastically. As the right femur of FSAC-KK 11888 has a total length of 0.625 m, our calculated whole-body CoM is more than one femur length cranial to the acetabulum. This is significant as it has been proposed that a whole-body CoM more than one femur length cranial to the acetabulum would make standing and moving bipedally impossible due to static instability[78]. Consequently, the whole-body CoM estimate for *Spinosaurus* implies a facultative, if not completely, quadrupedal gait on land and further supports our contention that *Spinosaurus* was highly adapted to an aquatic lifestyle.

8. Anatomical abbreviations

acdl, anterior centrodiapophyseal lamina;

c, centrum;

ca, caudal vertebra;

cdf, centrodiapophyseal fossa;

chva, chevron articulation;

chvh, chevron head;

cpol, centropostzygapophyseal lamina;

cprl, centroprezygapophyseal lamina;

hc, haemal canal;

na, neural arch;

ns, neural spine;

pcdl, posterior centrodiapophyseal lamina;

po, postzygapophysis;

pocdf, postzygapophyseal centrodiapophyseal fossa;

pocdl, postzygapophyseal centrodiapophyseal lamina;

podl, postzygodiapophyseal lamina;

posdf, postzygapophyseal spinodiapophyseal fossa;

posl, postspinal lamina;

pr, prezygapophysis;

prcdf, prezygapophyseal centrodiapophyseal fossa;

prcdl, prezygapophyseal centrodiapophyseal lamina;

prdl, prezygodiapophyseal lamina;

prsdf, prezygapophyseal spinodiapophyseal fossa;

prsl, prespinal lamina;

spdl, spinodiapophyseal lamina;

spol, spinopostzygapophyseal lamina;

spof, spinopostzygapophyseal fossa;

sprl, spinoprezygapophyseal lamina;

sprl-f, spinoprezygapophyseal lamina fossa;

tp, transverse process.

9. References

45. Martill, D. A., et al. A new Plattenkalk Konservat Lagerstätte in the Upper Cretaceous of Gara Sbaa, south-eastern Morocco. *Cretac. Res.* **32**, 433–446 (2011).

46. Ettachfini, El M. & Andreu, B. Le Cénomanien et le Turonien de la Plate-forme Préafricaine du Maroc. *Cretac. Res.* **25**, 277–302 (2004).

47. Ibrahim, N. et al. Dinosaur Footprints and Other Ichnofauna from the Cretaceous Kem Kem Beds of Morocco. *PloS ONE* **9**, e90751 (2014b).

48. Persons IV, W. S. & Currie, P. J. The tail of *Tyrannosaurus*: reassessing the size and locomotive importance of the *M. caudofemoralis* in non-avian theropods. *Anat. Rec.* **294**, 119–131 (2011).

49. Rauhut, O. W. M. The interrelationships and evolution of basal theropod dinosaurs. *Spec. Pap. Paleontol.* **69**, 1–213 (2003).

50. Novas, F. E., Dalla Vecchia, F. M., Pais D. F. Theropod pedal unguals from the Late Cretaceous of Morocco, Africa. *Rev. Mus. Argentino Cienc. Nat.* **7,** 167–175 (2005).

51. Tykoski, R. S. & Rowe, T. Ceratosauria. In The Dinosauria (Eds. Weishampel, D. B., Dodson, P. & Osmólska, H.) 47–70 (Berkeley, Univ. of California Press, 2004).

52. Wilson, J. A. Vertebral laminae in sauropods and other saurischian dinosaurs. *J. Vertebr. Paleontol.* **19**, 639-653 (1999).

53. Wilson, J. A. et al. A nomenclature for vertebral fossae in sauropods and other saurischian dinosaurs. *PLoS ONE* **6**, e17114 (2011).

54. Wilson, J. A. New vertebral laminae and patterns of serial variation in vertebral laminae of sauropod dinosaurs. *Contr. Mus. Paleontol. Univ. Michigan* **32**, 91–110 (2012).

55. Tereschenko, V. S. & Singer, T. Structural Features of Neural Spines of the Caudal Vertebrae of Protoceratopoids (Ornithischia: Neoceratopsia). *Paleontol. J.* **47**, 618–630. (2013).

56. Stromer, E. Wirbeltier-Reste der Baharije-Stufe (unterstes Cenoman). 13. Dinosauria. *Abh. bayer. Akad. Wissensch. Math.-Naturwiss* **22**, 1–79 (1934).

57. Mallison, H., Pittman, M. & Schwarz, D. Using crocodilian tails as models for dinosaur tails. *PeerJ* **3**, e1653 (2015).

58. Dal Sasso, C. & Maganuco, S. *Scipionyx samniticus* (Theropoda: Compsognathidae) from the Lower Cretaceous of Italy. Osteology, ontogenetic assessment, phylogeny, soft tissue anatomy, taphonomy and paleobiology. *Mem. Soc. Ital. Sci. Nat. Mus. Civ. Stor. Nat. Milano* **XXXVII**, 1–282 (2011).

59. Huchzermeyer, F. W. *Crocodiles: Biology, Husbandry and Diseases.* (Centre for Agricultural Bioscience International Publishing, 2003).

60. Horner, J. R., de Ricqlès, A. & Padian, K. Variation in dinosaur skeletochronology indicators: implications for age assessment and physiology. *Paleobiology* **25**, 295–304 (1999).

61. Horner, J. R., de Ricqlès, A. & Padian, K. Long bone histology of the hadrosaurid dinosaur *Maiasaura peeblesorum*: growth dynamics and physiology based on an ontogenetic series of skeletal elements. *J. Vertebr. Paleontol.* **20**, 115–129 (2000).

62. Chinsamy-Turan, A. The microstructure of dinosaur bone: deciphering biology with fine-scale techniques. *John Wiley & Sons*, 1-195 (2005).

63. Erickson, G. M. Assessing dinosaur growth patterns: a microscopic revolution. *Trends Ecol. & Evol.* **20**, 677-684 (2005).

64. Klein, N. & Sander, P. M. Bone histology and growth of the prosauropod dinosaur *Plateosaurus engelhardti* von Meyer, 1837 from the Norian bonebeds of Trossingen (Germany) and Frick (Switzerland). *Spec. Pap. Paleontol.* **77**, 169 (2007).

65. Hübner, T. R. Bone histology in *Dysalotosaurus lettowvorbecki* (Ornithischia: Iguanodontia)–variation, growth, and implications. *PLoS ONE* **7**, e29958 (2012).

66. Padian, K. & Lamm, E. T. (Eds.) *Bone histology of fossil tetrapods: advancing methods, analysis, and interpretation.* (Univ. of California Press, 2013).

67. Furstenburg, D. Focus op die lion (*Panthera leo*). *S. A. Hunter* **11070**, 24–25 (2012).

68. Furstenburg, D. Krokkodil (*Crocodylus niloticus*). *Game & Hunt* **14**, 6–12 (2008).

69. Mallison, H. & Wings, O. Photogrammetry in paleontology - A practical guide. *J. Paleontol. Techn.* **12**, 1–31 (2014).

70. Dal Sasso, C., Maganuco, S., Buffetaut, E. & Mendez, A. M. New information on the skull of the enigmatic theropod *Spinosaurus*, with remarks on its size and affinities. *J. Vertebr. Paleontol.* **25**, 888–896 (2005).

71. Bryant, H. N. & Russell, A. P. The role of phylogenetic analysis in the inference of unpreserved attributes of extinct taxa. *Philos. T. R. Soc B* **337**, 405–418 (1992).

72. Brassey, C. A. & Sellers, W. I. Scaling of convex hull volume to body mass in modern primates, non-primate mammals and birds. *PLoS ONE* **9**, e91691 (2014)**.**

73. Cott, H. B. Scientific results of an inquiry into the ecology and economic status of the Nile crocodile (*Crocodylus niloticus*) in Uganda and northern Rhodesia, *Trans. Zool. Soc. Lond.* **29**, 211–337 (1961).

74. Allen, V., Paxton, H. & Hutchinson, J. R. Variation in center of mass estimates for extant sauropsids and its importance for reconstructing inertial properties of extinct archosaurs. *Anat. Rec.* **292**, 1442–1461 (2009).

75. Bates, K. T., Manning, P. L., Hodgetts, D. & Sellers, W. I. Estimating mass properties of dinosaurs using laser imaging and 3D computer modelling. *PloS one* **4**, e4532 (2009).

76. Bates, K. T., Falkingham, P. L., Macaulay, S., Brassey, C. & Maidment, S. C. Downsizing a giant: re-evaluating *Dreadnoughtus* body mass. *Biol. let.* **11**, 20150215 (2015).

77. Henderson, D. M. & Snively, E. *Tyrannosaurus* en pointe: allometry minimised rotational inertia of large carnivorous dinosaurs. *Proc. R. Soc. B: Biological Sciences* **271**, 57–60 (2004).

78. Otero, A., Cuff, A. R., Allen, V., Sumner-Rooney, L., Pol, D. & Hutchinson, J. R. Ontogenetic changes in the body plan of the sauropodomorph dinosaur *Mussaurus patagonicus* reveal shifts of locomotor stance during growth. *Sci. rep.* **9**, 7614 (2019).